Environmental effects on the phase space dynamics and decoherence time scale of a charged particle in a Penning trap

2009 J. Phys. A: Math. Theor. 42 385302

(http://iopscience.iop.org/1751-8121/42/38/385302)

J. Phys. A: Math. Theor. **42** (2009) 385302 (13pp) doi:10.1088/1751-8113/42/38/385302

Environmental effects on the phase space dynamics and decoherence time scale of a charged particle in a Penning trap

M Genkin and E Lindroth

Department of Atomic Physics, University of Stockholm, Stockholm, Sweden

E-mail: genkin@physto.se

Received 5 June 2009, in final form 6 August 2009
Published 1 September 2009
Online at stacks.iop.org/JPhysA/42/385302

Abstract
We study the time evolution of a charged particle in a Penning trap in the framework of open quantum systems. The interaction with the environment is taken into account by imposing Lindblad operators which are linear in the canonical variables. For the special case of a proton in an asymmetric Penning trap, we compare the dynamics with earlier results obtained from the unitary time-dependent Schrödinger equation. A possibility of estimating the spatial decoherence time of the system is discussed, and approximate decoherence time scales are given for different ions.

PACS numbers: 03.65.−w, 03.65.Sq, 03.65.Yz, 37.10.Ty

1. Introduction

Penning traps provided an enormous improvement in the field of high-precision measurements performed on charged particles. Among many examples, one can mention their application in high-precision determination of fundamental constants [1, 2] and mass measurements, see e.g. [3, 4] for a recent detailed review. Penning traps are also used in the ATRAP and ATHENA projects [5, 6] at CERN aiming for production and, eventually, spectroscopy of cold antihydrogen. As a further exciting example, we would like to mention quantum information processing with traps, as suggested in [7], which was successfully demonstrated experimentally on beryllium [8] and calcium [9–12] ions in a linear Paul trap. Penning traps, however, also have certain experimental advantages in this context [13, 14], and schemes for their use in quantum computation have been recently proposed [15–19].

Penning traps are, however, not only indispensable in many experimental setups. The dynamics of a charged particle in a Penning trap shows interesting features also from a theoretical point of view. Since the Hamiltonian of such a system is quadratic in the canonical variables, some rather fundamental quantum mechanical aspects can be approached analytically. This was successfully explored during the past few years, e.g. in phase space dynamics calculations [20] or derivations of specific classes of coherent [21], squeezed [22], or Schrödinger cat [23, 24] states. In the present work, we demonstrate that the reduced dynamics is also analytically solvable in the presence of an environment, if certain conditions on the latter are imposed. While dissipation due to radiation damping or coupling to an external circuit are known to be quite weak [25], there are also other possible sources for dissipation and decoherence such as e.g. scattering off residual gas atoms (collisional decoherence), which motivated the present study.

The paper is organized as follows: in section 2, we present the model based on the Markovian master equation of Lindblad type [26] from which the equations of motion are derived, and give the solutions of the latter. In section 3, the special case of a proton in an asymmetric trap is considered, and the time evolution of the dispersions in coordinates and momenta is given explicitly in the zero temperature limit. Three particular initial states are considered: squeezed states as well as even and odd Schrödinger cat states, and the results for all three cases are compared to those obtained in [23] within a unitary picture, thus clearly illustrating the environmental effects. In section 4, we discuss how information about the decoherence of the system, induced by the presence of an environment, can be estimated and give approximate decoherence time scales for different charged particles. A brief summary is made in section 5.

2. Non-unitary equations of motion

The Hamiltonian of a charged particle with mass m and charge q in a Penning trap reads

$$H = \frac{p^2}{2m} + \frac{\omega_c}{2}(xp_y - yp_x) + \frac{m}{2}\left(\omega_x^2 x^2 + \omega_y^2 y^2 + \omega_z^2 z^2\right), \tag{1}$$

where $\omega_c = qB/m$ (B being the magnetic field strength in the trap) is the cyclotron frequency and ω_z the axial frequency, and the frequencies ω_x, ω_y are given by

$$\omega_x^2 = \frac{\omega_c^2}{4} - \frac{\omega_z^2}{2}(1+\beta), \tag{2a}$$

$$\omega_y^2 = \frac{\omega_c^2}{4} - \frac{\omega_z^2}{2}(1-\beta), \tag{2b}$$

where $-1 < \beta < 1$ is the asymmetry parameter. Here and in the following, the spin motion is completely separable from the dynamics and hence it is not considered in our calculations. To obtain the equations of motion in the presence of an environment, we solve the following Lindblad-type Markovian master equation [26] for the density matrix:

$$\frac{\mathrm{d}\rho}{\mathrm{d}t} = -\frac{\mathrm{i}}{\hbar}[H, \rho] + \frac{1}{2\hbar}\sum_j \left(\left[V_j\rho, V_j^\dagger\right] + \left[V_j, \rho V_j^\dagger\right]\right). \tag{3}$$

The Lindblad operators V_j are chosen to be linear superpositions of the canonical coordinates and momenta with complex coefficients a_{jk}, b_{jk}:

$$V_j = \sum_{k=1}^{3}(a_{jk}p_k + b_{jk}r_k), \qquad V_j^\dagger = \sum_{k=1}^{3}(a_{jk}^* p_k + b_{jk}^* r_k), \qquad j = 1, \ldots, 6, \tag{4}$$

where the number of the Lindblad operators is limited by the dimension of the problem at hand. One should mention that this general approach is, in fact, well known, especially in the field of nuclear physics where mostly one-dimensional [27–29] and two-dimensional

[30, 31] models of such form have been widely used to phenomenologically describe the damping of collective modes in deep-inelastc heavy ion collisions. The same formalism has also been used in several more general quantum mechanical discussions [32–37]. However, to the best of our knowledge, it has not been studied in connection with Penning traps before.

The coefficients a_{jk}, b_{jk} give rise to a number of phenomenological constants that appear in the equations of motion. The dynamics can be simplified if we make certain assumptions about the heat bath. In particular, we demand the system–environment interaction to be uniform, i.e. that the damping in a certain coordinate or momentum does not affect the time evolution of any other coordinate and momentum (and in the same way for the variances). To express these physical conditions technically, we define, in terms of the above coefficients, the vectors

$$\mathbf{a_k} = (a_{1k}, \dots, a_{6k})^{\mathrm{T}}, \qquad \mathbf{b_k} = (b_{1k}, \dots, b_{6k})^{\mathrm{T}}, \qquad k = 1, \dots, 3, \tag{5}$$

and introduce the scalar product

$$\langle \mathbf{f}, \mathbf{g} \rangle = \sum_{i=1}^{6} f_i^* g_i. \tag{6}$$

The relations to hold can then be written as follows:

$$\mathrm{Im}\langle \mathbf{a_k}, \mathbf{a_l} \rangle = 0, \qquad k, l = 1, \dots, 3, \tag{7a}$$

$$\mathrm{Im}\langle \mathbf{b_k}, \mathbf{b_l} \rangle = 0, \qquad k, l = 1, \dots, 3, \tag{7b}$$

$$\mathrm{Re}\langle \mathbf{a_k}, \mathbf{b_l} \rangle = 0, \qquad k, l = 1, \dots, 3, \tag{7c}$$

$$\mathrm{Im}\langle \mathbf{a_k}, \mathbf{b_l} \rangle = 0, \qquad \text{if} \quad k \neq l, \tag{7d}$$

$$\mathrm{Re}\langle \mathbf{a_k}, \mathbf{a_l} \rangle = 0, \qquad \text{if} \quad k \neq l, \tag{7e}$$

$$\mathrm{Re}\langle \mathbf{b_k}, \mathbf{b_l} \rangle = 0, \qquad \text{if} \quad k \neq l. \tag{7f}$$

For convenience, we introduce the following abbreviations for the non-vanishing scalar products above:

$$\lambda_k = -\mathrm{Im}\langle \mathbf{a_k}, \mathbf{b_k} \rangle, \qquad D_{r_k r_k} = \frac{\hbar}{2} \mathrm{Re}\langle \mathbf{a_k}, \mathbf{a_k} \rangle, \qquad D_{p_k p_k} = \frac{\hbar}{2} \mathrm{Re}\langle \mathbf{b_k}, \mathbf{b_k} \rangle. \tag{8}$$

They are often referred to as 'phenomenological dissipation constants' (λ_k) and 'diffusion coefficients' $\left(D_{r_k r_k}, D_{p_k p_k}\right)$. Another necessary assumption is that of weak coupling of the system to the environment since master equations of the form (3) are valid within this limit only [38]. In the given case, this means, for example, that the values λ_k should be much smaller than the typical frequencies of the considered system.

The equations of motion for the expectation values of an operator A can now be obtained by transforming the master equation (3) to the Heisenberg picture,

$$\frac{\mathrm{d}A}{\mathrm{d}t} = \frac{\mathrm{i}}{\hbar}[H, A] + \frac{1}{2\hbar} \sum_j \left(V_j^\dagger [A, V_j] + \left[V_j^\dagger, A\right] V_j\right), \tag{9}$$

and by introducing the vector of the phase space expectation values $\boldsymbol{\eta} = (\langle \mathbf{r} \rangle, \langle \mathbf{p} \rangle)^T$ and evaluating the commutators above for all of its components, the equations of motion for the first moments take the form

$$\frac{\mathrm{d}\boldsymbol{\eta}}{\mathrm{d}t} = \Lambda \boldsymbol{\eta}, \tag{10}$$

where Λ is the time evolution matrix

$$\Lambda = \begin{pmatrix} -\lambda_1 & -\omega_c/2 & 0 & 1/m & 0 & 0 \\ \omega_c/2 & -\lambda_2 & 0 & 0 & 1/m & 0 \\ 0 & 0 & -\lambda_3 & 0 & 0 & 1/m \\ -m\omega_x^2 & 0 & 0 & -\lambda_1 & -\omega_c/2 & 0 \\ 0 & -m\omega_y^2 & 0 & \omega_c/2 & -\lambda_2 & 0 \\ 0 & 0 & -m\omega_z^2 & 0 & 0 & -\lambda_3 \end{pmatrix}. \tag{11}$$

This corresponds to the result recently obtained for unitary time evolution in a symmetric ($\beta = 0$) Penning trap (see equation (8) in [21], where we identify $b = \omega_c/2$, $b^2 + \nu = \omega_x^2 = \omega_y^2$, $-2\nu = \omega_z^2$ and note that the mass was set to unity in the latter reference), where now the dissipative interaction with the environment gives rise to the diagonal elements of Λ. Given some initial conditions $\boldsymbol{\eta}(0)$, the solution of (10) is straightforward:

$$\eta(t) = e^{\Lambda t}\boldsymbol{\eta}(0). \tag{12}$$

The equations of motion for the second moments,

$$\sigma_{AB} = \sigma_{BA} = \tfrac{1}{2}\langle AB + BA\rangle - \langle A\rangle\langle B\rangle, \tag{13}$$

are derived from the Heisenberg representation of the master equation in the same manner, i.e. by inserting products of the components of η into (9) and evaluating the commutators. The result can be written in compact form by means of the covariance matrix σ_{ij}, where $i, j = 1, 2, 3$ correspond to the coordinates x, y, z and $i, j = 4, 5, 6$ to the momenta p_x, p_y, p_z:

$$\frac{d\sigma}{dt} = \Lambda\sigma + \sigma\Lambda^T + 2D, \tag{14}$$

where $D = \mathrm{diag}\left(D_{xx}, D_{yy}, D_{zz}, D_{p_xp_x}, D_{p_yp_y}, D_{p_zp_z}\right)$. This equation can be solved with the same ansatz as in the two-dimensional case [30, 31]:

$$\sigma(t) = \exp(\Lambda t)(\sigma(0) - \Gamma)(\exp(\Lambda t))^{\mathrm{T}} + \Gamma, \tag{15}$$

where $\sigma(0)$ is the initial covariance matrix and Γ is a symmetric matrix which is determined from the following system of linear equations:

$$\Lambda\Gamma + \Gamma\Lambda^T = -2D. \tag{16}$$

In the next section, we will compare the time evolution derived above with earlier results obtained from the time-dependent Schrödinger equation for a better illustration of the environmental effects.

3. Comparison with earlier results

We will consider the same example as in [23], where the motion of a proton in an asymmetric Penning trap was studied. In the latter reference, the parameters of the Hamiltonian (1) were taken as follows (see also table II in [25]):

$$\omega_c = 483.97\ \mathrm{MHz}, \qquad \omega_z = 63.22\ \mathrm{MHz}, \tag{17}$$

and the asymmetry parameter was chosen to be $\beta = 0.3$. We will also use the same units as in [23] throughout this section,

$$[t] = 4.21 \times 10^{-9}\ \mathrm{s}, \qquad [r] = 1.63 \times 10^{-8}\ \mathrm{m}, \qquad [p] = 6.48 \times 10^{-27}\ \mathrm{kg\ m\ s^{-1}}, \tag{18}$$

which implies that the proton mass and $\hbar$ are set to unity. Further, we note that due to the form of the Hamiltonian and the restrictions imposed on the environment, the motion in the

Table 1. Variances corresponding to the three classes of initial states considered here as they were found in [22, 23]. The abbreviations used below are $\omega_0^2 = 0.25\omega_c^2 - 0.5\omega_z^2$, $\Delta_+ = \tanh(|\alpha_x|^2 + |\alpha_y|^2)$, $\Delta_- = \coth(|\alpha_x|^2 + |\alpha_y|^2)$, where α_x, α_y are the in general complex mode amplitudes. Throughout this section we set $\alpha_x = \alpha_y = 1/3$. Note that the values in the second and third columns are dimensionless and have to be multiplied with the square of the characteristic length unit (for $\sigma_{r_i r_j}$), the square of the characteristic momentum unit (for $\sigma_{p_i p_j}$) and, respectively, with the characteristic unit of action (for $\sigma_{r_i p_j}$).

	Squeezed	Even Schrödinger cat	Odd Schrödinger cat
σ_{xx}	$\hbar/(m\omega_c)$	$\frac{\omega_0}{\omega_x}(\mathrm{Re}[\alpha_x(\alpha_x + \Delta_+\alpha_x^*)] + 0.5)$	$\frac{\omega_0}{\omega_x}(\mathrm{Re}[\alpha_x(\alpha_x + \Delta_-\alpha_x^*)] + 0.5)$
σ_{yy}	$\hbar/(m\omega_c)$	$\frac{\omega_0}{\omega_y}(\mathrm{Re}[\alpha_y(\alpha_y + \Delta_+\alpha_y^*)] + 0.5)$	$\frac{\omega_0}{\omega_y}(\mathrm{Re}[\alpha_y(\alpha_y + \Delta_-\alpha_y^*)] + 0.5)$
$\sigma_{p_x p_x}$	$\hbar m\omega_c/4$	$\frac{\omega_x}{\omega_0}(\mathrm{Re}[\alpha_x(-\alpha_x + \Delta_+\alpha_x^*)] + 0.5)$	$\frac{\omega_x}{\omega_0}(\mathrm{Re}[\alpha_x(-\alpha_x + \Delta_-\alpha_x^*)] + 0.5)$
$\sigma_{p_y p_y}$	$\hbar m\omega_c/4$	$\frac{\omega_y}{\omega_0}(\mathrm{Re}[\alpha_y(-\alpha_y + \Delta_+\alpha_y^*)] + 0.5)$	$\frac{\omega_y}{\omega_0}(\mathrm{Re}[\alpha_y(-\alpha_y + \Delta_-\alpha_y^*)] + 0.5)$
σ_{xy}	0	$\frac{\omega_0}{\sqrt{\omega_x\omega_y}}\mathrm{Re}[\alpha_x(\alpha_y + \Delta_+\alpha_y^*)]$	$\frac{\omega_0}{\sqrt{\omega_x\omega_y}}\mathrm{Re}[\alpha_x(\alpha_y + \Delta_-\alpha_y^*)]$
σ_{xp_x}	0	$\mathrm{Im}[\alpha_x(\alpha_x + \Delta_+\alpha_x^*)]$	$\mathrm{Im}[\alpha_y(\alpha_x + \Delta_-\alpha_x^*)]$
σ_{xp_y}	0	$\sqrt{\frac{\omega_y}{\omega_x}}\mathrm{Im}[\alpha_y(\alpha_x + \Delta_+\alpha_x^*)]$	$\sqrt{\frac{\omega_y}{\omega_x}}\mathrm{Im}[\alpha_y(\alpha_x + \Delta_-\alpha_x^*)]$
σ_{yp_x}	0	$\sqrt{\frac{\omega_x}{\omega_y}}\mathrm{Im}[\alpha_x(\alpha_y + \Delta_+\alpha_y^*)]$	$\sqrt{\frac{\omega_x}{\omega_y}}\mathrm{Im}[\alpha_x(\alpha_y + \Delta_-\alpha_y^*)]$
σ_{yp_y}	0	$\mathrm{Im}[\alpha_y(\alpha_y + \Delta_+\alpha_y^*)]$	$\mathrm{Im}[\alpha_y(\alpha_y + \Delta_-\alpha_y^*)]$
$\sigma_{p_x p_y}$	0	$\frac{\sqrt{\omega_x\omega_y}}{\omega_0}\mathrm{Re}[\alpha_x(-\alpha_y + \Delta_+\alpha_y^*)]$	$\frac{\sqrt{\omega_x\omega_y}}{\omega_0}\mathrm{Re}[\alpha_x(-\alpha_y + \Delta_-\alpha_y^*)]$

z-direction completely decouples from the dynamics in the xy-plane. Hence, the former reduces to a one-dimensional quantum oscillator with Lindbladian damping [27]. For the dynamics in the xy-plane, we assume the damping to be essentially in the cyclotron motion, and bearing in mind the imposed weak coupling limit, we set λ_1 and λ_2 to be of the order of $10^{-3}\omega_c$. For the diffusion coefficients, in general, the temperature-dependent expressions are discussed e.g. in [27, 29, 33],

$$D_{r_k r_k} = \frac{\hbar\lambda_k}{2m\omega_k}\coth\left(\frac{\hbar\omega_k}{2kT}\right), \qquad D_{p_k p_k} = \frac{\hbar\lambda_k m\omega_k}{2}\coth\left(\frac{\hbar\omega_k}{2kT}\right), \tag{19}$$

where T is the temperature and k the Boltzmann constant, but for simplicity we will consider the zero-temperature limit at this point, so that the diffusion coefficients become temperature independent:

$$D_{r_k r_k} = \frac{\hbar\lambda_k}{2m\omega_k}, \qquad D_{p_k p_k} = \frac{\hbar\lambda_k m\omega_k}{2}. \tag{20}$$

It should be mentioned that these coefficients cannot be chosen arbitrarily but have to obey some constraints which are related to the preservation of the positivity of the density matrix and the uncertainty relation [39]. The next step is to specify the initial conditions. Following [23], we will consider three different kinds of initial states: squeezed states as well as even and odd Schrödinger cat states. The initial variances corresponding to these states were found in [22, 23] and are summarized in table 1. Figures 1 and 2 show the calculated time evolution of the same dispersions as considered in [23] for different dissipation strengths and initial states. Our results coincide with those obtained therein in the limit $\lambda_1 = \lambda_2 \to 0$ (up to a numerical conversion factor in the time scale [40]), and at the same time the environmental effects are clearly visible in the case of non-vanishing λ_1, λ_2. They manifest themselves in a very natural way that one would expect, namely in the amplitude damping of the oscillations.

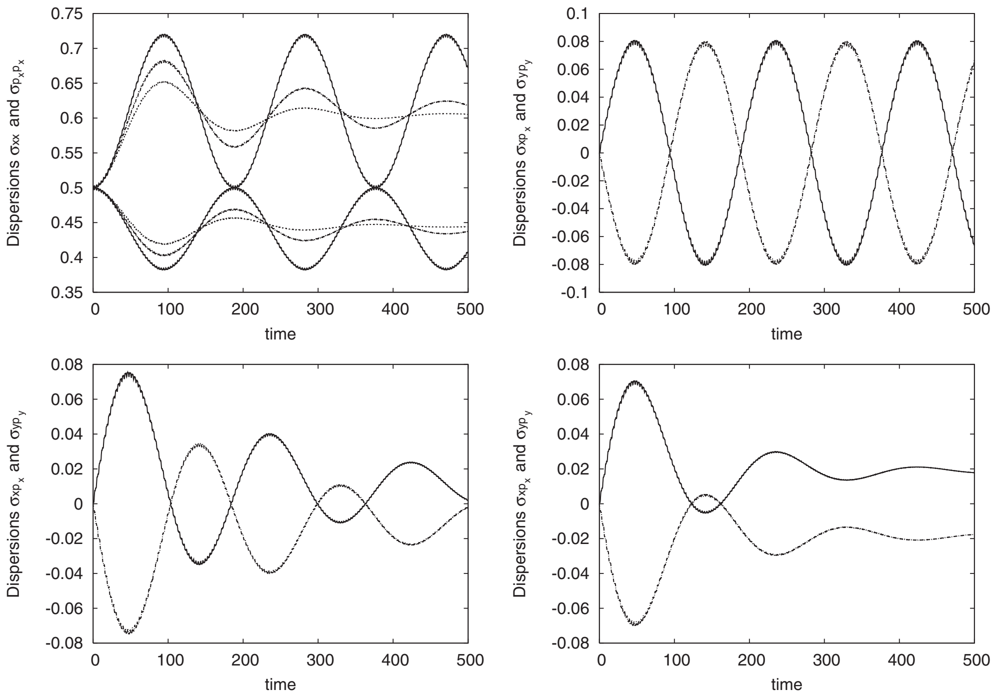

Figure 1. Time evolution of different dispersions for a proton in a Penning trap, initially prepared in a squeezed state. The upper-left panel shows the time evolution of the diagonal elements σ_{xx} (the three lower curves) and $\sigma_{p_x p_x}$ (the upper curves) in the limit $\lambda_1 = \lambda_2 = 0$ (solid lines) and for two different dissipation strengths: $\lambda_1 = \lambda_2 = 10^{-3}\omega_c$ (dashed lines) and $\lambda_1 = \lambda_2 = 2 \times 10^{-3}\omega_c$ (dotted lines). The other three panels show the corresponding time evolution of the off-diagonal elements σ_{xp_x} (solid lines) and σ_{yp_y} (dashed lines) for the same dissipation strengths, $\lambda_1 = \lambda_2 = 0$ (upper right), $\lambda_1 = \lambda_2 = 10^{-3}\omega_c$ (lower left) and $\lambda_1 = \lambda_2 = 2 \times 10^{-3}\omega_c$ (lower right).

4. Decoherence time scale

In the final part of the paper, we address the dynamics of spatial decoherence of an ion in a Penning trap. For that purpose, we assume the ion to be initially prepared in a Penning trap coherent state. Such a class of states was recently derived in [21] for a symmetric trap (i.e. $\beta = 0$ in (2)), and for simplicity we will assume a symmetric trap throughout this section as well. To find the initial values $\boldsymbol{\eta}(0)$ and $\sigma(0)$ corresponding to the Penning trap coherent states is straightforward [21, 41], and, as demonstrated in [41], the Penning trap coherent states have also the advantage to maximize the spatial degree of quantum decoherence. The latter is defined as the ratio of the coherence length, $l(t)$, of the reduced system to its ensemble width $W(t)$ [42–45]. It is not always possible to find an appropriate definition for these two quantities, but they are known for systems with Gaussian density matrices of the form

$$\rho(x, x', t) = \mathcal{N}(t) \exp\left(-A(t)(x - x')^2 - \mathrm{i}B(t)(x - x')(x + x') - C(t)\left(\frac{x + x'}{2}\right)^2\right), \quad (21)$$

where $\mathcal{N}(t)$ is a normalization factor. The coherence length and ensemble width are, in this case, given by the amplitudes of the diagonal $(x = x')$ and off-diagonal $(x = -x')$ elements

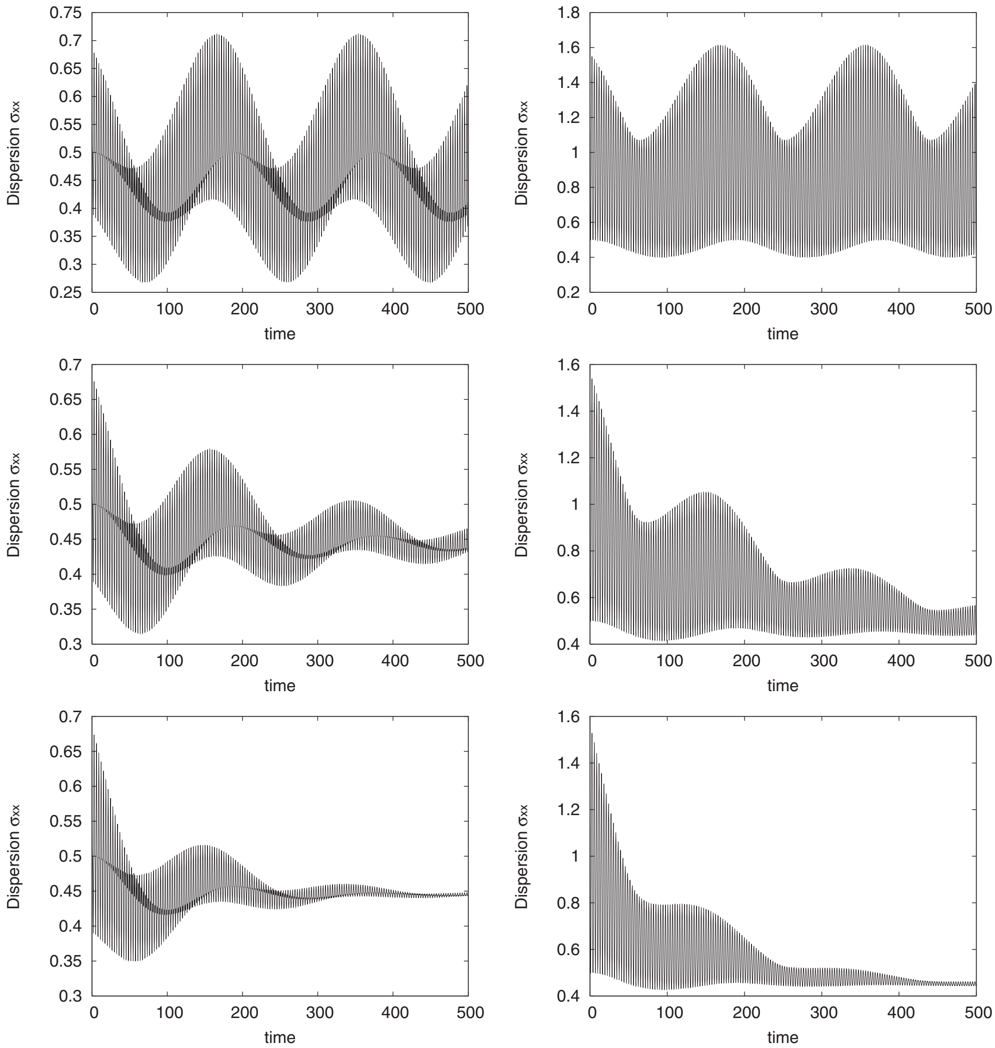

Figure 2. Time evolution of the dispersion σ_{xx} for a proton in a Penning trap, initially prepared in an even (left panels) or odd (right panels) Schrödinger cat state. The evolution is shown for three different dissipation strengths, from top to bottom: $\lambda_1 = \lambda_2 = 0$, $\lambda_1 = \lambda_2 = 10^{-3}\omega_c$ and $\lambda_1 = \lambda_2 = 2 \times 10^{-3}\omega_c$.

of the density matrix,

$$l(t) = \sqrt{\frac{1}{8A(t)}}, \qquad W(t) = \sqrt{\frac{1}{2C(t)}}, \tag{22}$$

and hence the decoherence degree becomes

$$\delta_{QD}(t) = \frac{l(t)}{W(t)} = \frac{1}{2}\sqrt{\frac{C(t)}{A(t)}}. \tag{23}$$

Since we are dealing with a quadratic Hamiltonian and the initial state is of Gaussian type, the Gaussian form remains preserved for all times and therefore we can directly adopt the definition above as a measure of spatial quantum decoherence. Furthermore, due to the structure of the Hamiltonian and the restrictions imposed on the Lindblad operators, the density matrix of the three-dimensional system $\hat{\rho}_{xyz}$ can be written as the direct product

$$\hat{\rho}_{xyz}(t) = \hat{\rho}_{xy}(t) \otimes \hat{\rho}_z(t). \tag{24}$$

Although the time scale of the motion in the z-direction is much slower than that of the motion in the xy-plane, the decoherence effects related to the z-motion will occur faster since the asymptotic decoherence degree in harmonic potentials scales as $\sim\tanh(\hbar\omega/(2kT))$ [43] and $\omega_z \ll \omega_{x,y}$. To investigate spatial decoherence in the xy-motion, we require the expression for $\hat{\rho}_{xy}(t)$ in the coordinate representation,

$$\langle x, y|\hat{\rho}_{xy}|x', y'\rangle(t) = \rho(x, x', y, y', t). \tag{25}$$

Since the time evolution of the first and second moments is known from (12) and (15), we can directly use the well-known result for Gaussian–Wigner functions in quadratic potentials [30, 46–48],

$$f_W(\mathbf{r}, \mathbf{p}, t) = \frac{1}{\sqrt{\det(2\pi\sigma(t))}} \exp\left(-\frac{1}{2}(\boldsymbol{\xi} - \boldsymbol{\eta}(t))^{\mathrm{T}}\sigma(t)^{-1}(\boldsymbol{\xi} - \boldsymbol{\eta}(t))\right), \tag{26}$$

to obtain the density matrix via the transformation

$$\langle\mathbf{r}|\hat{\rho}|\mathbf{r}'\rangle = \int \mathrm{d}\mathbf{p} \exp\left(\frac{\mathrm{i}}{\hbar}(\mathbf{p}(\mathbf{r} - \mathbf{r}'))\right) f_W((\mathbf{r} + \mathbf{r}')/2, \mathbf{p}, t). \tag{27}$$

Note that ξ denotes the phase space vector $\xi = (\mathbf{r}, \mathbf{p})^T$ in (26) while the vector $\eta(t)$ gives the expectation value of ξ at time t. The integral above can be performed analytically, which yields

$$\begin{aligned}\langle x, y|\hat{\rho}_{xy}|x', y'\rangle(t) = N \exp\Big[&-K_1(\Sigma_x - \langle x\rangle)^2 - K_2(\Sigma_y - \langle y\rangle)^2 - K_3(\Sigma_x - \langle x\rangle)(\Sigma_y - \langle y\rangle)\\ &-K_4\Delta_x^2 - K_5\Delta_y^2 + K_6\Delta_x\Delta_y + \mathrm{i}K_7(\Sigma_x - \langle x\rangle)\Delta_x + \mathrm{i}K_8(\Sigma_y - \langle y\rangle)\Delta_y\\ &+\mathrm{i}K_9(\Sigma_x - \langle x\rangle)\Delta_y + \mathrm{i}K_{10}(\Sigma_y - \langle y\rangle)\Delta_x + \frac{\mathrm{i}}{\hbar}(\langle p_x\rangle\Delta_x + \langle p_y\rangle\Delta_y)\Big].\end{aligned} \tag{28}$$

Here, the brackets $\langle\cdots\rangle$ denote expectation values and for convenience we introduce new coordinates,

$$\begin{aligned}\Sigma_x &= \frac{x + x'}{2}, \qquad \Delta_x = x - x',\\ \Sigma_y &= \frac{y + y'}{2}, \qquad \Delta_y = y - y'.\end{aligned} \tag{29}$$

The explicit form of the time-dependent factors $K_1, \ldots, K_{10}$ is given in the appendix together with the normalization factor N. For completeness, we also give the z-part of the density matrix:

$$\begin{aligned}\langle z|\hat{\rho}_z|z'\rangle(t) = \sqrt{\frac{1}{2\pi\sigma_{zz}}} \exp\Bigg[&-\frac{1}{2\sigma_{zz}}\left(\frac{z + z'}{2} - \langle z\rangle\right)^2 - \frac{\sigma_{zz}\sigma_{p_zp_z} - \sigma_{zp_z}^2}{2\hbar^2\sigma_{zz}}(z - z')^2\\ &+\frac{\mathrm{i}\sigma_{zp_z}}{\hbar\sigma_{zz}}\left(\frac{z + z'}{2} - \langle z\rangle\right)(z - z') + \frac{\mathrm{i}}{\hbar}\langle p_z\rangle(z - z')\Bigg].\end{aligned} \tag{30}$$

Note that in (28) and (30), the expectation values $\langle r_i \rangle$, $\langle p_i \rangle$ and the variances are functions of time. We can now easily identify the coherence length and ensemble width according to (22) in the x and y components in (28):

$$l_x(t) = \sqrt{\frac{1}{8K_1}}, \qquad l_y(t) = \sqrt{\frac{1}{8K_2}},$$
$$W_x(t) = \sqrt{\frac{1}{2K_4}}, \qquad W_y(t) = \sqrt{\frac{1}{2K_5}}. \tag{31}$$

If, in addition, we demand the dissipation to be equal in both coordinates, i.e. $\lambda_1 = \lambda_2$, then, since we consider a symmetric trap, the coherence lengths and ensemble widths will also be equal at all times ($l_x(t) = l_y(t)$, $W_x(t) = W_y(t)$), which, according to (23), allows us to define a single spatial decoherence degree for the cyclotron motion

$$\delta_{QD}(t) = \frac{1}{2}\sqrt{\frac{K_1}{K_4}} = \frac{1}{2}\sqrt{\frac{K_2}{K_5}}. \tag{32}$$

Since the system is initially prepared in a Penning trap coherent state, we have, as shown in [41], $\delta_{QD}(0) = 1$, and with increasing time the quantum coherence decays until it has reached a final asymptotic value. We would like to emphasize that, contrary to the previous section, we consider a finite temperature in the diffusion coefficients (19) which is crucial for the decoherence dynamics. Thus, even in the presence of an environment a coherent state remains coherent for all times if the reservoir temperature is zero [43]. Figure 3 shows the time evolution of the decoherence degree for different ions in the mass range from 4 amu to 129 amu at $T = 4$ K which is a typical operation temperature in most Penning trap experiments. A comparison with the results of the previous section indicates that the decoherence time scale is several orders of magnitude shorter than the relaxation time scale, which is a rather common behaviour. This agrees with the thumb rule for estimating the ratio of the two time scales [45]

$$\frac{\tau_{\mathrm{rel}}}{\tau_{\mathrm{dec}}} \approx \frac{\sigma_{xx}}{L_{\mathrm{dB}}^2}, \tag{33}$$

where σ_{xx} is the typical spatial spread of the system and

$$L_{\mathrm{dB}}^2 = \frac{\hbar^2}{2mkT} \tag{34}$$

is the squared thermal de Broglie wave length. Indeed, inserting some typical parameters ($m = 50$ amu, $B = 5$ T, $T = 4$ K, $q = e$, $\omega_c = eB/m$, $\sigma_{xx} = \hbar/(m\omega_c)$) we find the ratio to be of the order of 10^5, which is about the ratio of the time scales in figures 1 and 2, that display a relaxation process, to that of figure 3 that displays decoherence dynamics. In this context, it should also be stated that this ratio becomes astronomically large for macroscopic systems, and only for very few systems (e.g. some solid state devices like quantum dots) both processes can occur on the same timescale. However, within the model adopted here to describe environmental effects, the spatial decoherence turns out to be quite sensitive with respect to the temperature, so that the decoherence time can be significantly prolonged by cooling the setup down to the mK regime.

5. Summary

We studied the dynamics of a charged particle in a Penning trap within the Lindblad theory, which allows us to incorporate environmental effects in a phenomenological way. We derived

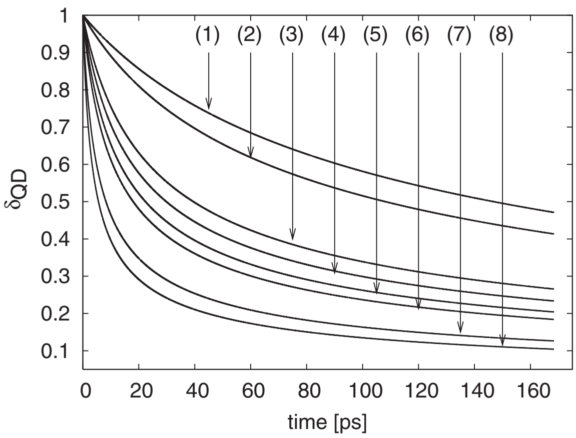

Figure 3. The time evolution of the spatial decoherence parameter, shown for different ions in the mass range from 4 amu to 129 amu. The ions are listed in table 2 together with the experiment from which the frequencies and magnetic field strengths were taken. The dissipation strength was taken to be $\lambda_1 = \lambda_2 = 1.0 \times 10^{-3}\omega_c$ at a temperature of $T = 4$ K.

Table 2. The description of curves (1)–(8) in figure 3, showing the ions for which the calculations were performed and the experiment from which the input parameters, i.e. the frequencies and magnetic field strengths, were taken.

Curve	(1)	(2)	(3)	(4)	(5)	(6)	(7)	(8)
Ion	$^{4}He^{2+}$	$^{6}Li^{+}$	$^{18}O^{+}$	$^{24}Mg^{11+}$	$^{32}S^{+}$	$^{40}Ca^{19+}$	$^{87}Rb^{2+}$	$^{129}Xe^{5+}$
Magnetic field (T)	6.0	7.0	8.5	4.7	8.5	4.7	8.5	8.5
Experiment	[49]	[50]	[51]	[52]	[53]	[54]	[55]	[56]

the equations of motion for the first and second moments and presented an analytical solution of the latter. For the particular example of a proton moving in a Penning trap, we investigated the time-behaviour of the dispersions and made a comparison to earlier results. It is found that in the limit of vanishing environmental coupling strength, the dynamics agrees with the one obtained from the time-dependent Schrödinger equation without dissipation while with increasing coupling strength the oscillations in the dispersions become more and more damped and approach finite asymptotic values. We also suggested a possibility of estimating the spatial decoherence time scale for ions in a Penning trap using recent experimental setups as examples. Within the model we used, the decoherence time scale at a temperature of $T = 4$ K is found to be about $\tau_{\mathrm{dec}} \approx 100$ ps. This is much shorter than the estimated relaxation time which is of the order of 1 μs in the considered weak coupling case $\lambda_k \approx 10^{-3}\omega_c$. The model presented here is limited by the Markovian condition and therefore cannot be used to describe strongly damped dynamics, but, apart from its simplicity, it has the advantage that the environmental effects can be taken into account without being specified explicitly. At the same time, additional information is necessary to relate the phenomenological parameters to physical quantities, e.g. in the case of collisional decoherence reliable scattering rates off the residual gas atoms are required to find appropriate values for the dissipation constants λ_k. The temperature of the heat bath, however, can be taken into account through the diffusion coefficients, which considerably influences the decoherence time scale.

Acknowledgments

We thank Professor Reinhold Schuch for explanations about the experimental aspects and Professor Shahen Hacyan for the kind private communication concerning earlier results. This work was supported by the Göran Gustafsson Foundation and the Swedish research council (VR).

Appendix. Explicit form of the factors and normalization in equation (28)

The time-dependent normalization factor N and the time-dependent amplitudes $K_1, \ldots, K_{10}$ in (28) can be explicitly given by means of the covariance submatrix of the xy-motion,

$$S = \begin{pmatrix} \sigma_{xx} & \sigma_{xy} & \sigma_{xp_x} & \sigma_{xp_y} \\ \sigma_{yx} & \sigma_{yy} & \sigma_{yp_x} & \sigma_{yp_y} \\ \sigma_{p_xx} & \sigma_{p_xy} & \sigma_{p_xp_x} & \sigma_{p_xp_y} \\ \sigma_{p_yx} & \sigma_{p_yy} & \sigma_{p_yp_x} & \sigma_{p_yp_y} \end{pmatrix}, \tag{A.1}$$

the time evolution of which is directly obtained from the full covariance matrix σ (see (15)). Denoting by $C = S^{-1}$, the inverse of the above matrix and its elements by c_{ij}, the explicit expression for the normalization reads

$$N = \sqrt{\frac{4\pi^2}{\det(2\pi S)\left(\mathrm{c}_{33}\mathrm{c}_{34} - \mathrm{c}_{34}^2\right)}} \tag{A.2}$$

and the amplitudes are given by

$$K_1(t) = \frac{c_{11}}{2} + \frac{c_{13}c_{14}c_{34} - \frac{1}{2}\left(c_{13}^2c_{44} + c_{14}^2c_{33}\right)}{c_{33}c_{44} - c_{34}^2}, \tag{A.3}$$

$$K_2(t) = \frac{c_{22}}{2} + \frac{c_{23}c_{24}c_{34} - \frac{1}{2}\left(c_{23}^2c_{44} + c_{24}^2c_{33}\right)}{c_{33}c_{44} - c_{34}^2}, \tag{A.4}$$

$$K_3(t) = c_{12} + \frac{c_{34}(c_{13}c_{24} + c_{14}c_{23}) - (c_{13}c_{23}c_{44} + c_{14}c_{24}c_{33})}{c_{33}c_{44} - c_{34}^2}, \tag{A.5}$$

$$K_4(t) = \frac{c_{44}}{2\hbar^2\left(c_{33}c_{44} - c_{34}^2\right)}, \tag{A.6}$$

$$K_5(t) = \frac{c_{33}}{2\hbar^2\left(c_{33}c_{44} - c_{34}^2\right)}, \tag{A.7}$$

$$K_6(t) = \frac{c_{34}}{\hbar^2\left(c_{33}c_{44} - c_{34}^2\right)}, \tag{A.8}$$

$$K_7(t) = \frac{c_{34}c_{14} - c_{44}c_{13}}{\hbar\left(c_{33}c_{44} - c_{34}^2\right)}, \tag{A.9}$$

$$K_8(t) = \frac{c_{34}c_{23} - c_{24}c_{33}}{\hbar\left(c_{33}c_{44} - c_{34}^2\right)}, \tag{A.10}$$

$$K_9(t) = \frac{c_{34}c_{13} - c_{14}c_{33}}{\hbar\left(c_{33}c_{44} - c_{34}^2\right)}, \tag{A.11}$$

$$K_{10}(t) = \frac{c_{34}c_{24} - c_{23}c_{44}}{\hbar\left(c_{33}c_{44} - c_{34}^2\right)}. \tag{A.12}$$

References

[1] Van Dyck R S Jr, Schwinberg P B and Dehmelt H G 1987 *Phys. Rev. Lett.* **59** 26
[2] Gabrielse G, Fei X, Orozco L A, Tjoelker R L, Haas J, Kalinowsky H, Trainor T A and Kells W 1990 *Phys. Rev. Lett.* **65** 1317
[3] Blaum K 2006 *Phys. Rep.* **425** 1
[4] Blaum K, Nagy S and Werth G 2009 *J. Phys. B: At. Mol. Opt. Phys.* **42** 154015
[5] Gabrielse G *et al* 2008 *Phys. Rev. Lett.* **100** 113001
[6] Madsen N *et al* 2005 *Phys. Rev. Lett.* **94** 033403
[7] Cirac J I and Zoller P 1995 *Phys. Rev. Lett.* **74** 4091
[8] Monroe C, Meekhof D M, King B E, Itano W M and Wineland D J 1995 *Phys. Rev. Lett.* **75** 4714
[9] Schmidt-Kaler F, Gulde S, Riebe M, Deuschle T, Kreuter A, Lancaster G, Becher C, Eschner J, Häffner H and Blatt R 2003 *J. Phys. B: At. Mol. Opt. Phys.* **36** 623
[10] Riebe M, Kim K, Schindler P, Monz T, Schmidt P O, Körber T K, Hänsel W, Häffner H, Roos C F and Blatt R 2006 *Phys. Rev. Lett.* **97** 220407
[11] Benhelm J, Kirchmair G, Roos C F and Blatt R 2008 *Phys. Rev.* A **77** 062306
[12] Monz T, Kim K, Hänsel W, Riebe M, Villar A S, Schindler P, Chwalla M, Hennrich M and Blatt R 2009 *Phys. Rev. Lett.* **102** 040501
[13] Powell H F, Segal D M and Thompson R C 2002 *Phys. Rev. Lett.* **89** 093003
[14] Koo K, Sudbery J, Segal D M and Thompson R C 2004 *Phys. Rev.* A **69** 043402
[15] Ciaramicoli G, Marzoli I and Tombesi P 2003 *Phys. Rev. Lett.* **91** 017901
[16] Ciaramicoli G, Marzoli I and Tombesi P 2004 *Phys. Rev.* A **70** 032301
[17] Castrejón-Pita J R and Thompson R C 2005 *Phys. Rev.* A **72** 013405
[18] Zurita-Sánchez J R and Henkel C 2008 *New J. Phys.* **10** 083021
[19] Marzoli I *et al* 2009 *J. Phys. B: At. Mol. Opt. Phys.* **42** 154010
[20] Fernández D J and Nieto L M 1991 *Phys. Lett.* A **157** 315
[21] Fernández D J and Velázquez M 2009 *J. Phys. A: Math. Theor.* **42** 085304
[22] Hacyan S 1996 *Phys. Rev.* A **53** 4481
[23] Castaños O, Hacyan S, López-Peña R and Man'ko V I 1998 *J. Phys. A: Math. Gen.* **31** 1227
[24] Massini M, Fortunato M, Mancini S, Tombesi P and Vitali D 2000 *New J. Phys.* **2** 20
[25] Brown L S and Gabrielse G 1986 *Rev. Mod. Phys.* **58** 233
[26] Lindblad G 1976 *Commun. Math. Phys.* **48** 119
[27] Sandulescu A and Scutaru H 1987 *Ann. Phys.* **173** 277
[28] Antonenko N V, Ivanova S P, Jolos R V and Scheid W 1994 *J. Phys. G: Nucl. Part. Phys.* **20** 1447
[29] Adamian G G, Antonenko N V and Scheid W 1999 *Nucl. Phys.* A **645** 376
[30] Sandulescu A, Scutaru H and Scheid W 1987 *J. Phys. A: Math. Gen.* **20** 2121
[31] Genkin M and Scheid W 2007 *J. Phys. G: Nucl. Part. Phys.* **34** 441
[32] Isar A, Sandulescu A and Scheid W 1999 *Phys. Rev.* E **60** 6371
[33] Palchikov Y V, Adamian G G, Antonenko N V and Scheid W 2000 *J. Phys. A: Math. Gen.* **33** 4265
[34] Isar A, Sandulescu A and Scheid W 2000 *Eur. Phys. J.* D **12** 3
[35] Isar A and Scheid W 2002 *Phys. Rev.* A **66** 042117
[36] Genkin M and Lindroth E 2008 *J. Phys. A: Math. Theor.* **41** 425303
[37] Ozorio de Almeida A M, de M Rios P and Brodier O 2009 *J. Phys. A: Math. Theor.* **42** 0653061
[38] Karrlein R and Grabert H 1997 *Phys. Rev.* E **55** 153
[39] Dekker H and Valsakumar M C 1984 *Phys. Lett.* A **104** 67
[40] Hacyan S 2009, Private communication
[41] Genkin M and Lindroth E 2009 *J. Phys. A: Math. Theor.* **42** 275305
[42] Morikawa M 1990 *Phys. Rev.* D **42** 2929
[43] Isar A and Scheid W 2007 *Physica* A **373** 298
[44] Joos E, Zeh H D, Kiefer C, Giulini D, Kupsch J and Stamatescu I O 2003 *Decoherence and the Appearance of a Classical World in Quantum Theory* (Berlin: Springer)
[45] Schlosshauer M 2007 *Decoherence and the Quantum-to-Classical Transition* (Berlin: Springer)
[46] Wang M C and Uhlenbeck G E 1945 *Rev. Mod. Phys.* **17** 323
[47] Agarwal G S 1971 *Phys. Rev.* A **4** 739
[48] Dodonov V V and Manko O V 1985 *Physica* A **130** 353
[49] Van Dyck R S Jr, Zafonte S L, Van Liew S, Pinegar D B and Schwinberg P B 2004 *Phys. Rev. Lett.* **92** 220802
[50] Heavner T P, Jefferts S R and Dunn G H 2001 *Phys. Rev.* A **64** 062504

[51] Redshaw M, Mount B J and Myers E G 2009 *Phys. Rev.* A **79** 012507
[52] Bergström I, Björkhage M, Blaum K, Bluhme H, Fritioff T, Nagy S and Schuch R 2003 *Eur. Phys. J.* D **22** 41
[53] Shi W, Redshaw M and Myers E G 2005 *Phys. Rev.* A **72** 022510
[54] Nagy S, Fritioff T, Solders A, Schuch R, Björkhage M and Bergström I 2006 *Eur. Phys. J.* D **39** 1
[55] Bradley M P, Porto J V, Rainville S, Thompson J K and Pritchard D E 1999 *Phys. Rev. Lett.* **83** 4510
[56] Redshaw M, Mount B J and Myers E G 2009 *Phys. Rev.* A **79** 012506